Priority Report

Cancer Research

Inflammation Triggers Zeb1-Dependent Escape from Tumor Latency

Jasmine M. De Cock[1,2], Tsukasa Shibue[1], Anushka Dongre[1], Zuzana Keckesova[1], Ferenc Reinhardt[1], and Robert A. Weinberg[1,2,3]

Abstract

The emergence of metastatic disease in cancer patients many years or decades after initial successful treatment of primary tumors is well documented but poorly understood at the molecular level. Recent studies have begun exploring the cell-intrinsic programs, causing disseminated tumor cells to enter latency and the cellular signals in the surrounding nonpermissive tissue microenvironment that maintain the latent state. However, relatively little is known about the mechanisms that enable disseminated tumor cells to escape cancer dormancy or tumor latency. We describe here an *in vivo* model of solitary metastatic latency in the lung parenchyma. The induction of a localized inflammation in the lungs, initiated by lipopolysaccharide treatment, triggers the awakening of these cells, which develop into macroscopic metastases. The escape from latency is dependent on the expression of Zeb1, a key regulator of the epithelial-to-mesenchymal transition (EMT). Furthermore, activation of the EMT program on its own, as orchestrated by Zeb1, is sufficient to incite metastatic outgrowth by causing carcinoma cells to enter stably into a metastasis-initiating cell state. *Cancer Res; 76(23); 6778–84. ©2016 AACR.*

Introduction

Metastasis-related mortality for breast cancer patients often occurs many years after treatment of their primary tumors. The cause(s) of latency of disseminated tumor cells (DTC) and the mechanism(s) leading to eruption of metastatic disease remain poorly understood (1, 2). At present, it is unknown whether each DTC has the potential to act as a founder cell of a metastasis or whether this function is reserved for specialized DTCs deemed "metastasis-initiating cells" (MIC). Recent studies of cancer dormancy have focused on the cell-intrinsic traits that maintain DTCs in the dormant state (3–5). Although inflammation is widely recognized as a hallmark of cancer and has been shown to predispose certain tissues to form primary tumors, far less is known of the role of inflammation in metastatic colonization, that is, in enabling the outgrowth of already extravasated cells in distant tissues.

Although certain studies have suggested that a preinflamed microenvironment can enhance the ability of DTCs to extravasate and subsequently colonize a metastatic site (6–9), it has not been determined whether an inflamed microenvironment in the vicinity of already extravasated latent DTCs can enable their escape from growth arrest. We therefore sought to determine whether inflammation, provoked through the administration of lipopolysaccharide (LPS) in mice, could trigger the activation of the previously silent epithelial–mesenchymal transition (EMT) program in latent DTCs. We postulated that the activation of the EMT program, which can be induced by a diverse array of signals, including those associated with inflammation, could cause latent DTCs to generate MICs and grow into overt metastases.

Materials and Methods

Cell culture

Mouse mammary carcinoma cell lines (D2A1, 67NR, and 168 FARN) and TS/A were gifts from F.R. Miller (retired, Molecular Therapeutics Program, Barbara Ann Karmanos Cancer Institute and Departments of Oncology and Pathology, Wayne State University School of Medicine, Detroit, MI) and P.L. Lollini (Department of Experimental Diagnostic and Specialty Medicine, University of Bologna, Bologna, Italy), respectively. Cells were maintained as described previously (10) and were not authenticated since the first acquisition. For activating tetracycline-inducible gene expression, cells were treated with 1 μg/mL doxycycline hyclate (Sigma-Aldrich).

Plasmids and lentiviral infections

Mouse Snail, Twist1, and Zeb1 cDNAs obtained from Open Biosystems were subcloned into FUW-LPT2 lentiviral vector (modified from FUW-tetO) with puromycin resistance gene. pMMP-LucNeo, carrying coding sequences for luciferase and neomycin phosphotransferase, were obtained from Dr. Rosalind Segal (Dana Farber Cancer Institute, Boston, MA).

pLKO-puro shZeb1 vectors (shZeb1_A and shZeb1_B) were used as described previously (10). Cells were seeded at 5.0×10^5 cells per 10 cm dish and transduced 24 hours later with virus in the presence of 5 μg/mL polybrene (EMD Millipore) and selected with 4 μg/mL puromycin.

[1]Whitehead Institute for Biomedical Research, Cambridge, Massachusetts. [2]Department of Biology, Massachusetts Institute of Technology, Cambridge, Massachusetts. [3]MIT Ludwig Center for Molecular Oncology, Cambridge, Massachusetts.

Corresponding Author: Robert A. Weinberg, Whitehead Institute for Biomedical Research, 9 Cambridge Center, WHTH-367, Cambridge, MA 02142. Phone: 617-258-5159; Fax: 617-258-5213; E-mail: weinberg@wi.mit.edu

doi: 10.1158/0008-5472.CAN-16-0608

AACR

Cell proliferation assay

Cells were seeded at 1.0×10^6 into 10-cm dishes and counted using Vi-CELL Cell Viability Analyzer (Beckman Coulter). Cells (1.0×10^3) were seeded onto 96-well plates in triplicate; viability was measured using CellTiter-Glo (Promega).

Matrigel on-top

The Matrigel on-top (MoT) culture was performed as described elsewhere (10).

Quantitative RT-PCR

Total RNA was isolated using the RNeasy Plus Mini Kit (Qiagen). Reverse transcription was performed with High-Capacity cDNA Reverse Transcription Kit (Life Technologies). mRNA levels were measured with gene-specific primers using SYBR Green I Master Mix (Roche) on a Roche LightCycler 480 system (Roche). Relative expression levels were normalized to β-actin. The PCR primers for Snail, Twist, Zeb1, and β-actin have been described elsewhere (10).

Immunoblotting

Western blots were performed as described previously (10) using the following antibodies: Snail (Cell Signaling Technology), Twist (Abcam), Zeb1 (Cell Signaling Technology), E-cadherin (Cell Signaling Technology), GAPDH (Cell Signaling Technology), and actin (Cell Signaling Technology).

Animals

Animal studies were conducted following the MIT Committee on Animal Care protocol (1014-109-17). Tumor cells (1.0×10^5), unless otherwise indicated, suspended in Matrigel 1:1 were implanted into the mammary fat pad of BALB/c mice. Tumor incidence and weight were measured 6 to 8 weeks postinjection. Cells (1.0×10^5), resuspended in 100 μL of PBS, were injected into the lateral tail vein; alternatively, 8.0×10^4 cells were injected into the left ventricle. Doxycycline-treated water contained 2 mg/mL doxycycline and 10 mg/mL sucrose.

Acute lung injury

Escherichia coli LPS type 055:B5 (Sigma Aldrich) was delivered by intraperitoneal injection at 2 mg/kg. Mice were bled retro-orbitally to obtain peripheral white blood cell counts. Anti-Ly6G antibody clone 1A8 (200 μg/mouse; Bio X Cell) was injected intraperitoneally one day prior LPS treatment and 24 hours after LPS treatment to deplete neutrophils. Anti-CCL2 antibody (200 μg/mouse, Bio X Cell) was injected intraperitoneally 6 hours after LPS treatment and again 24 hours after LPS treatment to deplete circulating monocytes and macrophages. Matching isotype hamster IgG (Bio X Cell) served as a control antibody.

Quantification of lung metastases

Whole-lung images were taken using a fluorescence dissection microscope (Leica MZ12). Colonies visible at 0.8× magnification of objective lens under fluorescence microscopy were counted as macrometastases.

Histology

Lungs were fixed in 4% paraformaldehyde, paraffin embedded, and stained with hematoxylin and eosin. Sections were imaged at 20× with the Aperio slide scanner (Leica Biosystems).

Bioluminescent imaging

Mice were anesthetized with 2.5% isoflurane and injected intraperitoneally with 165 mg/kg of body weight D-luciferin (Caliper Life Sciences) and imaged in a Xenogen IVIS 10 minutes after D-luciferin injection; data were analyzed using Living Image Software version 4.3.1 (Caliper Life Sciences).

Flow cytometry

Lungs were minced and incubated in DME + DNAse + collagenase A (Roche) rotating at 37°C for 2 hours. Dissociated lungs were then washed twice with PBS and filtered through a 70 and 40 μm cell strainer. Cells were stained with CD45 FITC (eBioscience), CD11b PerCP-Cyanine 5.5 (eBioscience), F480 PE-Cyanine7 (Affymetrix), CCR2 APC-Cy7 (BioLegend), Ly6C e450 (Affymetrix), CD45 PE-Cyanine7 (Affymetrix), CD11b PerCP-Cyanine5.5 (eBioscience), Ly6C e450 (Affymetrix), Ly6G FITC (BioLegend), CD29 (Affymetrix), and CD24 (Affymetrix). After incubating on ice for 45 minutes, cells were washed twice in PBS with 0.1% BSA, acquired on a Fortessa (BD Biosciences) and analyzed using FACSDiva (BD Biosciences).

Results

To generate a model of metastatic dormancy, highly metastatic murine D2A1 mammary carcinoma cells (11) prelabeled with the CSFE vital dye were injected via the tail vein into mice, leading to many being trapped in the lungs. Five days later, label-retaining cells, which had therefore failed to proliferate within the lungs, were enriched by FACS, expanded *in vitro*, and reinjected into mice (Fig. 1A). After 10 successive cycles of such *in vivo* selection, latent cells (denoted D2A1-d) retained the ability to form primary tumors upon orthotopic injection of 10^5 cells into the mammary fat pad, yet failed to proliferate within the lung parenchyma 4 weeks after tail vein injection (Supplementary Tables S1 and S2). However, a significant reduction in primary tumor growth was seen when only 10^4 D2A1-d cells were implanted, suggesting a growth deficiency *in vivo* when compared with parental D2A1 cells (Supplementary Fig. S1A and S1B). While the D2A1-d cells fail to proliferate within the lung parenchyma after 4 weeks, D2A1-d cells could indeed be recovered from dissociated lung tissue following introduction into 2D culture *ex vivo*, indicating that latent D2A1-d cells were still present in a viable form long after tail vein injection.

Previous work demonstrated that induced expression of EMT-inducing transcription factors (EMT-TF) in carcinoma cells enables them to extend filopodium-like protrusions (FLP), ensuring proliferation within the lung parenchyma following extravasation (10). This suggested that defective FLP formation might provide a mechanistic explanation of the observed postextravasation tumor latency of D2A1-d cells. However, we found no difference in the ability of the D2A1-d and parental D2A1 cells to extend FLPs (Supplementary Fig. S1C), despite the reduced or absent expression of the EMT-TFs Snail, Twist, and Zeb1 (Fig. 1B; ref. 12). Nonetheless, we hypothesized that the EMT program might still play a role in triggering the awakening of latent DTCs via an FLP-independent mechanism.

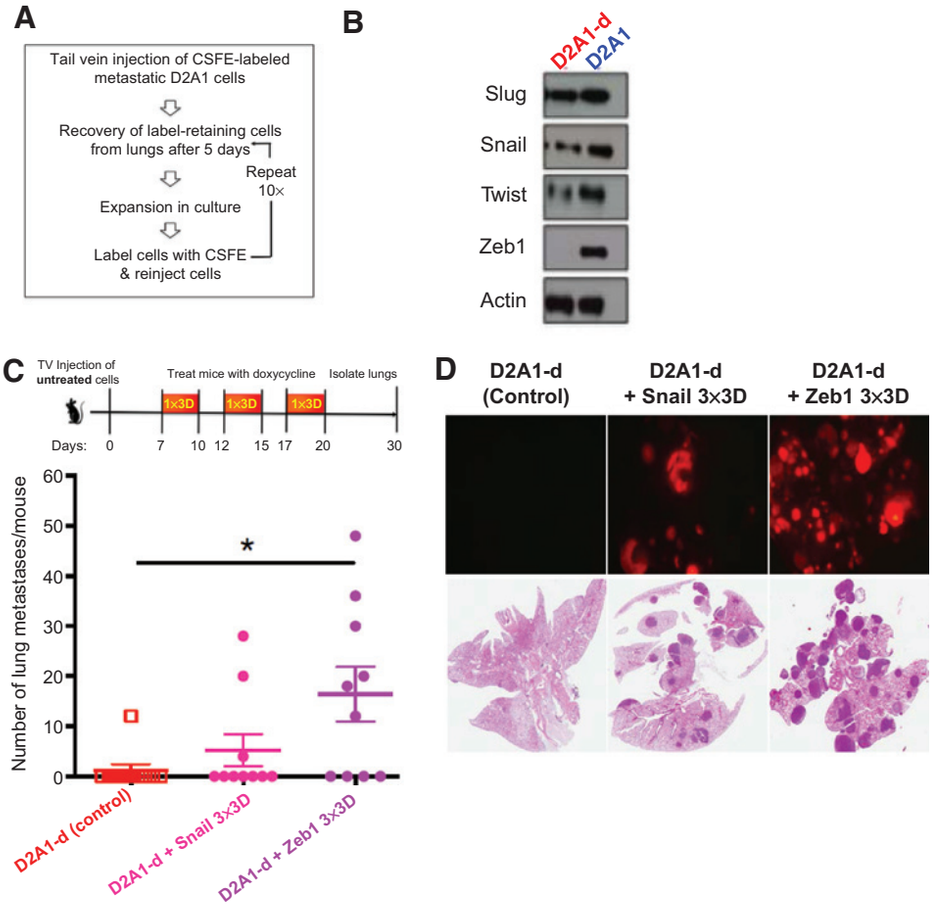

Figure 1.
Zeb1 expression is sufficient to awaken latent DTCs. **A,** Schematic of *in vivo* strategy. **B,** Western blot analysis for D2A1-d and parental D2A1 cell lines. **C,** Schematic of *in vivo* strategy. TV, tail vein. Quantification of lung metastases using fluorescent dissection microscope at ×0.8 magnification. Data, mean ± SEM; $n = 10$. *, $P < 0.02$ by Student t test. **D,** Representative fluorescent images of whole lungs and hematoxylin and eosin staining of histologic sections.

To determine whether induction of an EMT program in latent DTCs would be sufficient to enable their escape from tumor latency, we used a doxycycline-inducible vector to express either Snail, Twist, or Zeb1 in D2A1-d cells (Supplementary Fig. S2A). No proliferative advantage was conferred on cells carrying the inducible EMT-TFs *in vitro* (Supplementary Fig. S2B).

We injected untreated D2A1-d cells harboring doxycycline-inducible vectors into the tail vein of mice, waited 7 days to achieve a postextravasation latent state, and then treated mice with doxycycline to determine whether the EMT program could reactivate metastatic growth in the lungs. In more detail, we used two alternative treatment schedules for inducing expression of the EMT-TFs. In initial experiments, we exposed mice to doxycycline continuously for 2 weeks; in subsequent experiments, we exposed mice to three periodic 3-day-long feedings of doxycycline.

As we found, the alternating interval treatment schedule was more productive for the induction of lung metastases in the case of D2A1-d + Zeb1 cells. Thus, continuous doxycycline treatment yielded on average eight metastases per lung (Supplementary Fig. S2D), while interval treatment generated 16 metastases (Fig. 1C and D). In the case of D2A1-d + Snail cells, both treatment protocols yielded the same number of metastases per lung, and no metastases were observed in the case of D2A1-d + Twist cells.

To determine whether the EMT program could awaken DTCs that experienced a longer period of latency, mice injected with D2A1-d + Snail cells were treated with doxycycline 3 weeks after tail vein injection (Supplementary Fig. S2E). Five weeks postinjection, mice carrying D2A1-d + Snail cells and treated with doxycycline developed on average 29 metastases per lung, while mice that remained untreated developed on average 15 metastases per lung. Although the latent D2A1-d cells retained a measure of metastasis-initiating ability, we deemed the observed 2-fold increase in metastasis formation (taken together with observations presented elsewhere in this report) to be significant and indicative of an ability of Snail to awaken otherwise latent D2A1-d cells.

To determine whether the EMT program had reprogrammed D2A1-d cells to a metastasis-initiating state in a cell-heritable manner, we retrieved D2A1-d cells from EMT-induced metastases and reinjected them via the tail vein into naïve hosts. Mice injected with these retrieved cells developed more than 200 lung metastases upon secondary passaging (Fig. 2A). Hence, EMT-TF expression *in vivo* promoted the acquisition of heritable MIC traits in previously latent DTCs.

Although the EMT program has been shown to generate cancer stem cell–like cells as gauged by an enhanced primary tumor-forming ability, it has been unclear whether the EMT program is also associated with the formation of MICs. We used murine stem cell–surface markers (10, 13) to conduct *in vitro* analyses on D2A1-d and parental cells. This revealed distinct CD24/CD29 profiles in the various cell populations (Fig. 2B). Thus, parental

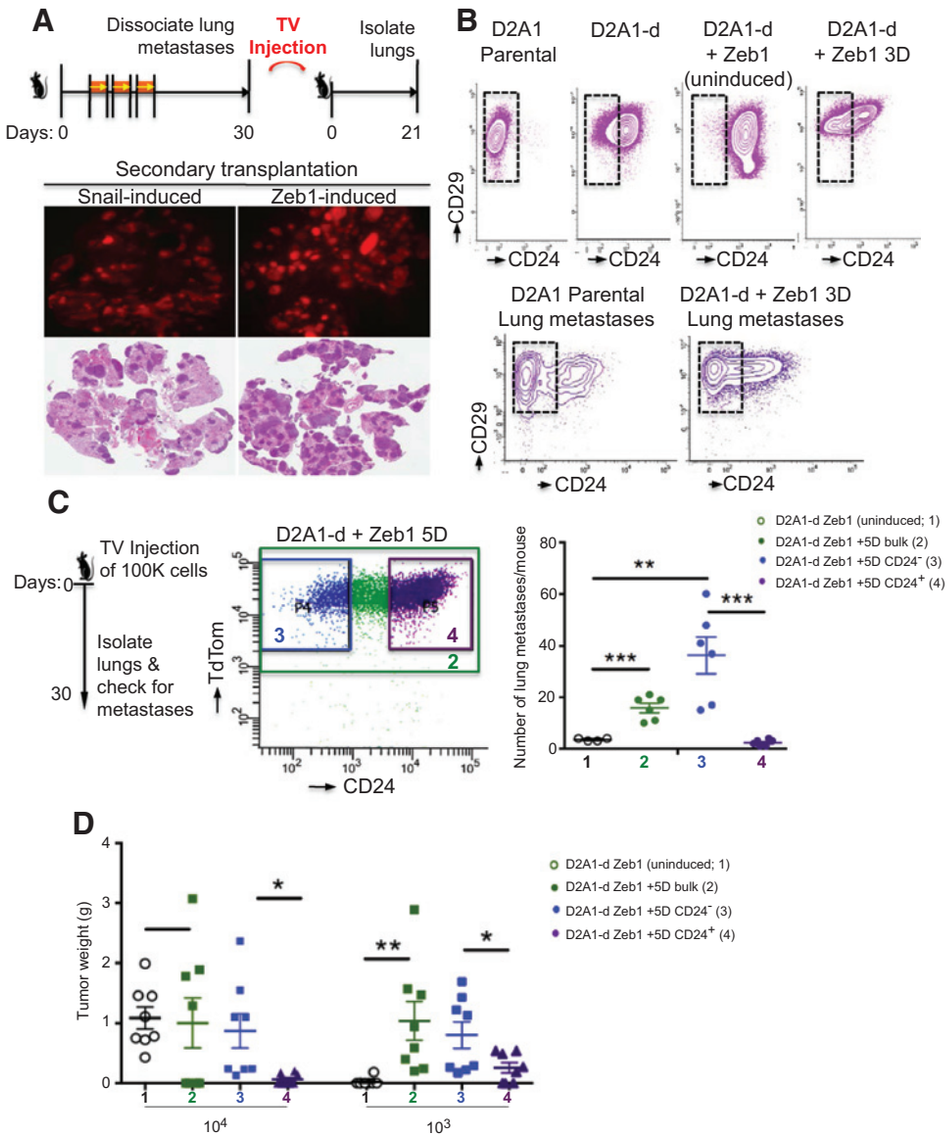

Figure 2.
Zeb1 expression generates MICs. **A,** Schematic of *in vivo* strategy. Fluorescent images and representative hematoxylin and eosin staining of whole lungs; $n = 6$. TV, tail vein. **B,** Flow cytometry analysis of CD29 and CD24 cell-surface expression of D2A1-d, parental D2A1, and D2A1-d + Zeb1 after 5 days of doxycycline treatment and tumor cells isolated from Zeb1-induced lung metastases and D2A1 lung metastases. **C,** Schematic of *in vivo* strategy. Quantification of lung metastases visible at ×0.8 magnification. Data, mean ± SEM; $n = 10$. **, $P < 0.07$; ***, $P < 0.001$ by Student t test. **D,** Orthotopic tumor weights of mice as described in **C** at dilution of 10^4 and 10^3 cells, respectively. ns, not significant.

D2A1 cells displayed a $CD29^+CD24^-$ marker profile (indicative of a more stem-like state), while D2A1-d cells exhibited a distinct $CD29^+CD24^+$ profile. However, upon expression of Zeb1 *in vitro*, D2A1-d + Zeb1 cells markedly shifted toward a $CD29^+CD24^-$ profile, which was also observed in the Zeb1-induced metastases (Fig. 2B).

When we sorted the $CD24^+$ and $CD24^-$ cells from *in vitro* Zeb1-induced D2A1-d cells and injected each population into the tail vein of mice, mice injected with the Zeb1-induced $CD29^+CD24^-$ cells formed an average of 36 metastases per mouse, whereas the $CD29^+CD24^+$ cells developed on average 2 metastases per mouse (Fig. 2C). While both the $CD29^+CD24^-$ and $CD29^+CD24^+$ cell populations were able to form orthotopic tumors, there was a significant difference in tumor-initiating frequencies and tumor weights between both cell populations (Fig. 2D; Supplementary Table S3; ref. 14). Because this difference was not as significant as the large difference observed in their respective abilities to form metastatic tumors in the lungs, the $CD29^+CD24^-$ marker profile could serve to enrich MICs in this cell line, enabling the isolation of a distinct subpopulation of tumor-initiating cells that could tumor initiate at the sites of formation of both primary tumors and metastases.

The EMT program can be activated by heterotypic signals under various physiologic and pathologic states (12). Although inflammation has been shown to contribute to primary tumor progression, the role of inflammation in metastatic colonization is poorly understood (15, 16). Recent studies have suggested that a preinflamed microenvironment in the lungs can enhance the ability of DTCs to subsequently colonize a metastatic site (7–9). We, in contrast, wished to explore an alternative scenario in which carcinoma cells arrive in an initially normal lung microenvironment and only thereafter experience proinflammatory signals. Thus, we hypothesized that an inflamed tissue microenvironment might release EMT-inducing signals, which in turn might spawn the activation of the EMT program in latent DTCs, leading to active proliferation and metastatic colonies.

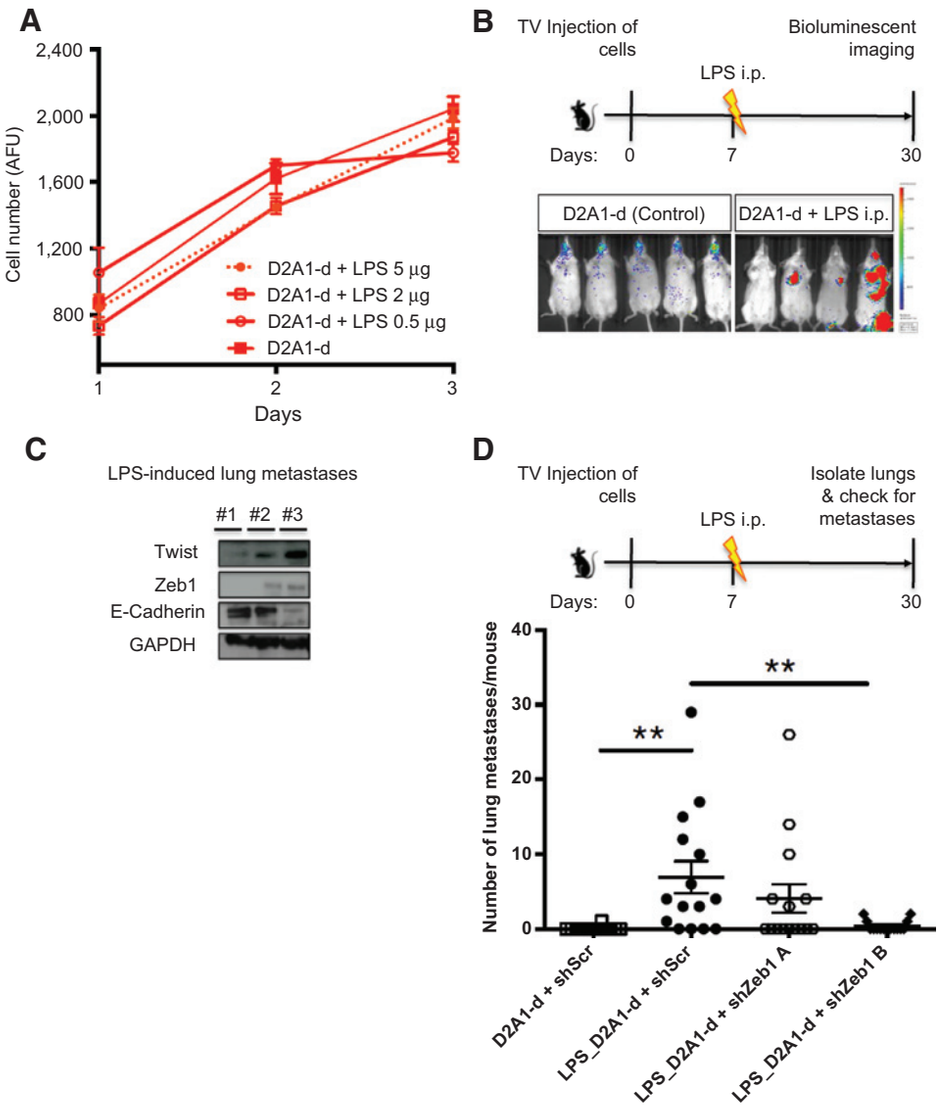

Figure 3.
LPS-induced inflammation awakens latent DTCs. **A,** *In vitro* CellTiter-Glo proliferation assay of D2A1-d in the presence or absence of 0.5, 2, and 5 μg/mL of LPS; $n = 3$. **B,** Schematic depiction of *in vivo* strategy. TV, tail vein. Representative luminescent images of mice previously injected with D2A1-d cells that received LPS intraperitoneally (i.p.). **C,** Pooled tumor cells isolated from lung metastases of three individual mice following LPS treatment were analyzed for the expression of E-cadherin, Twist, and Zeb1 by Western blot analysis. Mice are labeled "1," "2," and "3." **D,** Quantification of lung metastases at ×0.8 magnification. Data, mean ± SEM; $n = 10$. **, $P < 0.005$ by Student *t* test.

To test this notion, we first injected D2A1-d cells via the tail vein and thereafter treated mice with LPS, an agent used to provoke pulmonary inflammation (Fig. 3A and B and Supplementary Fig. S3A; ref. 17). Within 4 weeks, the mice that had been exposed to LPS carried on average seven lung metastases, while the control mice exhibited at most one metastasis.

To determine whether this result was idiosyncratic to the D2A1-d cells, we sought to extend this result using other weakly metastatic murine carcinoma cell lines. Mice injected with 67NR cells and treated one week later with LPS formed on average 10 metastases per mouse, while LPS-untreated mice injected with 67NR cells developed on average four metastases (Supplementary Fig. S3B and C).

D2A1-d cells retrieved from the LPS-induced lung metastases expressed elevated levels of the Twist and Zeb1 EMT-TFs, consistent with a causal association of the EMT program with induced metastatic outgrowth, as D2A1-d cells do not express these EMT-TFs under routine conditions (Fig. 3C). To test whether LPS-induced metastatic outgrowth was dependent upon the activation of an EMT program within the latent tumor cells, we first injected mice with D2A1-d cells carrying an shZeb1 vector; one week later, we treated these mice with LPS. Cells experiencing 90% knockdown of Zeb1 expression (shZeb1_B) yielded a 26% incidence of lung tumors, whereas cells experiencing only a 50% to 80% knockdown (shZeb1_A) yielded a tumor incidence of 40%. These incidence rates contrasted with those of cells bearing the control shRNA, in which 75% of mouse hosts developed metastases (Fig. 3D; Supplementary Table S4).

Of additional interest was the nature of the host cells that mediated the activation of the EMT program in the carcinoma cells. We excluded the contribution of the adaptive immune system by performing experiments in NOD/SCID mice. Thus, treating NOD/SCID mice injected with D2A1-d cells with LPS provoked metastatic outgrowth, yielding an average of 10 metastases per lungs, while the LPS-untreated mice developed on average three metastases per lungs (Supplementary Fig. S3D). These observations argued against the involvement of the

adaptive immune system in the observed eruption of LPS-induced metastases.

LPS is known to activate neutrophils, macrophages, and endothelial cells via toll-like receptor 4 signaling. To determine whether neutrophils, which are recruited in large numbers to the lungs following LPS treatment, contribute to metastatic outgrowth, we treated mice with anti-Ly6G antibody to eliminate these immunocytes. Only one mouse injected with D2A1-d cells + anti-Ly6G antibody and treated thereafter with LPS developed a metastasis, while the mice injected with D2A1-d cells + control IgG antibody and treated with LPS developed on average four lung metastases per mouse (Fig. 4A and B). Although there was an approximately 50% reduction in the number of neutrophils following control anti-IgG treatment as compared with the baseline level of neutrophils in the lungs (Fig. 4A), this was not sufficient to abrogate lung metastasis formation, thereby suggesting that there may exist a threshold of the number of neutrophils required to facilitate metastatic outgrowth. However, mice treated with neutralizing antibody against macrophages and treated thereafter with LPS developed on average three lung metastases per mouse as compared with the mice treated with LPS and control anti-IgG that developed on average four lung metastases per mouse, suggesting that macrophages are not essential for LPS-induced metastatic outgrowth (Fig. 4B).

To determine whether these results were specific to the lungs, we injected D2A1-d cells into mice via intracardiac injection and treated these mice one week later with LPS via intraperitoneal injection. Both control mice and LPS-treated mice developed adrenal gland metastases, while bone metastases were only apparent in LPS-treated mice (Fig. 4C).

Discussion

Although a preinflamed tissue microenvironment has been shown to foster subsequent metastatic outgrowth (7–9), to our knowledge, this is the first example of a study exploring the

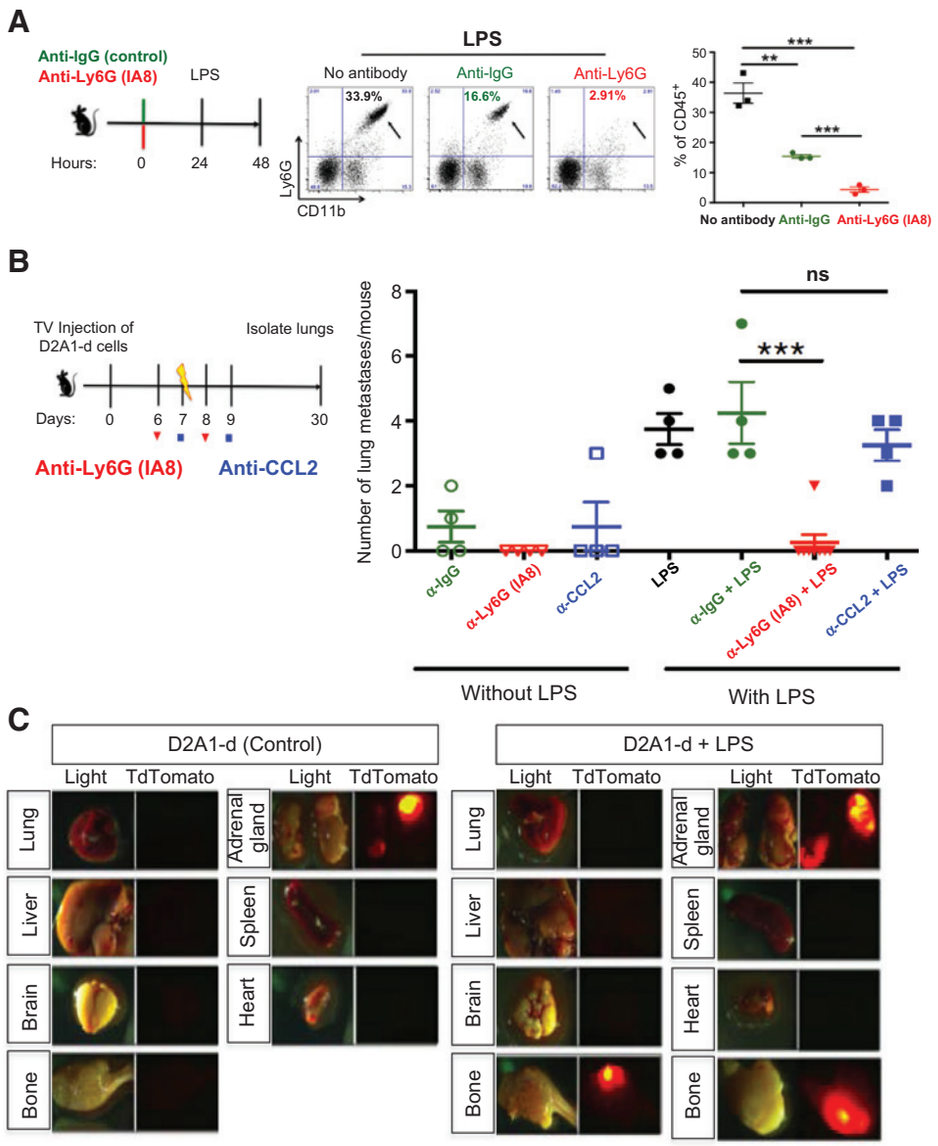

Figure 4.
Neutrophil depletion inhibits reactivation of latent DTCs. **A,** Schematic of neutrophil depletion in the lungs following a single injection of anti-Ly6G antibody after 48 hours. Percentage of $Ly6G^+$ $CD11b^+$ cells in total $CD45^+$ cells in lungs 48 hours after matched-control IgG antibody or anti-Ly6G antibody administration. **, $P = 0.0035$. **B,** Schematic of neutrophil or macrophages depletion strategy following LPS treatment in mice. ns, not significant; TV, tail vein. Quantification of lung metastases at ×0.8 magnification; $n = 4$ to 8. ***, $P < 0.0003$ by Student t test. ns, not significant. **C,** Representative images of whole-body tumor distribution of untreated or LPS-treated mouse following intracardiac injection of D2A1-d cells; 60% of LPS-treated mice developed bone metastases; $n = 12$.

effects of inflammation on previously seeded, latent DTCs. Although we were unable to determine the precise molecular mechanism leading to the awakening of latent DTCs by neutrophils, we would suggest that the activation of the EMT program within the carcinoma cells may depend in part on direct cell signaling between the latent DTCs and neutrophils, achieved either by the release of EMT-inducing cytokines, through the release of neutrophil-derived proteases (8), or both. Moreover, monocytes and macrophages recruited by neutrophils may well complement and augment the activating effects of the latter cells. Attesting to the possible generality of the identified mechanism, LPS-induced inflammation enabled not only colonization of the lungs, but also of the bone. Although our study focused on a single inflammatory agent, it is highly plausible that other proinflammatory stimuli could similarly ignite the escape of metastatic tumor latency. Moreover, we would suggest that the current work represents only the first of a number of diverse experimental models of DTC awakening that will be developed in the future, some of which may depend on quite different molecular mechanisms and signaling pathways to trigger the eruption of previously unapparent metastatic deposits.

Disclosure of Potential Conflicts of Interest

No potential conflicts of interest were disclosed.

Authors' Contributions

Conception and design: J.M. De Cock, Z. Keckesova, R.A. Weinberg
Development of methodology: J.M. De Cock, T. Shibue
Acquisition of data (provided animals, acquired and managed patients, provided facilities, etc.): J.M. De Cock, A. Dongre, F. Reinhardt
Analysis and interpretation of data (e.g., statistical analysis, biostatistics, computational analysis): J.M. De Cock, A. Dongre
Writing, review, and/or revision of the manuscript: J.M. De Cock, R.A. Weinberg
Administrative, technical, or material support (i.e., reporting or organizing data, constructing databases): J.M. De Cock
Study supervision: Z. Keckesova, R.A. Weinberg

Acknowledgments

We thank K.J. Kah, X. Ye, B. Bierie, A. Spiegel, and J. Froese for experimental assistance and reagents; R. Goldsby, J. Krall, S. Iyer, and W.A. Whyte for critical reading of the manuscript; J. Lees, R. Hynes, and members of the Weinberg laboratory for discussions; and P. Wisniewski, C. Zollo, and S. Malstrom for assistance with FACS and bioluminescent imaging acquisition. R.A. Weinberg is an American Cancer Society Research Professor and a Daniel K. Ludwig Cancer Research Professor.

Grant Support

R.A. Weinberg received support from Breast Cancer Research Foundation, NIH (P01 CA080111, R01 CA 078461, and U54 CA163109), and the Ludwig Center for Molecular Oncology.

Received March 2, 2016; revised June 19, 2016; accepted July 18, 2016; published OnlineFirst August 16, 2016.

References

1. Aguirre-Ghiso JA. Models, mechanisms and clinical evidence for cancer dormancy. Nat Rev Cancer 2007;7:834–46.
2. Giancotti F. Mechanisms governing metastatic dormancy and reactivation. Cell 2013;155:750–64.
3. Oskarsson T, Acharyya S, Zhang XH, Vanharanta S, Tavazoie SF, Morris PG, et al. Breast cancer cells produce tenascin C as a metastatic niche component to colonize the lungs. Nat Med 2011; 17:867–74.
4. Wendt MK, Taylor MA, Schiemann BJ, Schiemann WP. Down-regulation of epithelial cadherin is required to initiate metastatic outgrowth of breast cancer. Mol Biol Cell 2011;22:2423–35.
5. Gao H, Chakraborty G, Lee-Lim AP, Mo Q, Decker M, Vonica A, et al. The BMP inhibitor Coco reactivates breast cancer cells at lung metastatic sites. Cell 2012;150:764–79.
6. Ghajar CM, Peinado H, Mori H, Matei IR, Evason KJ, Brazier H, et al. The perivascular niche regulates breast tumour dormancy. Nat Cell Biol 2013;15:807–17.
7. Bouchard G, Bouvette G, Therriault H, Bujold R, Saucier C, Paquette B. Pre-irradiation of mouse mammary gland stimulates cancer cell migration and development of lung metastases. Br J Cancer 2013; 109:1829–38.
8. El Rayes T, Catena R, Lee S, Stawowczyk M, Joshi N, Fischbach C, et al. Lung inflammation promotes metastasis through neutrophil protease-mediated degradation of Tsp-1. Proc Natl Acad Sci U S A 2015;112: 16000–5.
9. Cox TR, Bird D, Baker AM, Barker HE, Ho MW, Lang G, et al. LOX-mediated collagen crosslinking is responsible for fibrosis-enhanced metastasis. Cancer Res 2013;73:1721–32.
10. Shibue T, Brooks MW,Weinberg RA. An integrin-linked machinery of cytoskeletal regulation that enables experimental tumor initiation and metastatic colonization. Cancer Cell 2013;4:381–98.
11. Morris VL, Tuck AB, Wilson SM, Percy D, Chambers AF. Tumor progression and metastasis in murine D2 hyperplastic alveolar nodule mammary tumor cell lines. Clin Exp Metastasis 1993;11:103–12.
12. Thiery JP, Acloque H, Huang RYJ, Nieto MA. Epithelial-mesenchymal transitions in development and disease. Cell 2009;139:871–90.
13. Visvader JE, Smith GH. Murine mammary epithelial stem cells: discovery, function, and current status. Cold Spring Harb Perspect Biol 2011;3: a004879.
14. Hu Y, Smyth GK. ELDA: extreme limiting dilution analysis for comparing depleted and enriched populations in stem cell and other assays. J Immunol Methods 2009;347:70–8.
15. Coussens LM, Werb Z. Inflammation and cancer. Nature 2002;420:860–7
16. Atsumi T, Singh R, Sabharwal L, Bando H, Meng J, Arima Y, et al. Inflammation amplifier, a new paradigm in cancer biology. Cancer Res 2014;74:8–14.
17. Brandolini L, Asti C, Ruggieri V, Intilangelo A, Pellegrini L, Chiusaroli R, et al. Lipopolysaccharide-induced lung injury in mice. II. Evaluation of functional damage in isolated parenchyma strips. Pulm Pharmacol Ther 2000;13:71–8.